High-performance Titanium Alloys and Lattice Structures

High-performance Titanium Alloys and Lattice Structures:

Design, Processing and Mechanical Properties

Edited by

Yuhua Li and Laichang Zhang

Cambridge
Scholars
Publishing

High-performance Titanium Alloys and Lattice Structures:
Design, Processing and Mechanical Properties

Edited by Yuhua Li and Laichang Zhang

This book first published 2025

Cambridge Scholars Publishing

Lady Stephenson Library, Newcastle upon Tyne, NE6 2PA, UK

British Library Cataloguing in Publication Data
A catalogue record for this book is available from the British Library

Copyright © 2025 by Yuhua Li, Laichang Zhang and contributors

All rights for this book reserved. No part of this book may be reproduced, stored in a retrieval system, or transmitted, in any form or by any means, electronic, mechanical, photocopying, recording or otherwise, without the prior permission of the copyright owner.

ISBN: 978-1-0364-4937-7
ISBN (Ebook): 978-1-0364-4938-4

TABLE OF CONTENTS

Preface vii

Contributors viii

Chapter 1 1
Categorization and Metallurgy of Titanium Alloys
Lai-Chang Zhang, Yuhua Li and Hongyi Ma

Chapter 2 40
Principles of Heat Treatment in Titanium Alloys
Dingmeng Xu and Peng Cao

Chapter 3 81
Beta-Type Titanium Alloys
Xin Wang, Yuhua Li, Yujie Yuan and Lai-Chang Zhang

Chapter 4 116
NiTi Alloys
Yuhua Li, Xin Wang, Yujie Yuan and Laichang Zhang

Chapter 5 150
Antibacterial Copper-Bearing Titanium Alloys
Kunmao Li, Shengfeng Zhou and Laichang Zhang

Chapter 6 187
High Strength and Low Yield Ratio Titanium Alloys
Diao-Feng Li, Chun-Guang Bai, Zhi-Qiang Zhang, Nan Li and Rui Yang

Chapter 7 214
Titanium Matrix Composites
Qingsong Mei and Xinlu Wang

Chapter 8 264
Laser Additive Manufacturing of Titanium Alloys
Chaolin Tan and Jinlong Su

Chapter 9 327
Mechanical Performance of Beta Ti-Nb Based Alloys Produced by Laser Powder Bed Fusion
Jincheng Wang, Yuhua Li, Yujing Liu and Lai-Chang Zhang

Chapter 10 362
Directed Energy Deposition of Titanium Alloys
Hua Tan, Wei Fan and Fengying Zhang

Chapter 11 400
Microstructure Manipulation of Ti-6Al-4V during Additive Manufacturing
Zhonggang Sun and Guoqing Dai

Chapter 12 443
Titanium Lattice Structures
Xin Wang, Chengliang Yang, Yuhua Li, Yujie Yuan and Lai-Chang Zhang

Chapter 13 474
Titanium Alloy Graded Lattice Structures
Lei Yang, Jiefei Huang and Hao Zhou

Chapter 14 536
Friction Stir Processing/Welding of Titanium Alloys: Process, Microstructure and Properties
Yuting Lv, Yan Wang, Yulong Shi, Wentang Deng, Wenlong Xie and Xiao Kong

Chapter 15 589
Micro-Arc Oxidation of Titanium Alloys and Their Applications as Biomaterials
Fengcang Ma, Ping Liu and Xiaohong Chen

Chapter 16 659
Electroshocking Treatment of Titanium Alloys
Jian Zhou, Chaoyi Ding, Chang Liu, Yan Wen and Lechun Xie

PREFACE

The reduction of CO_2 and pollutant emissions in transportation related industries can be addressed using high-performance lightweight alloys or porous structures with optimized strength-to-weight ratio. Nowadays, extensive endeavors have been made in designing and manufacturing high-strength lightweight alloys (e.g. titanium) and lattice structures. Therefore, this book emphasizes the importance of high-performance titanium alloys and lattice structures in the campaign against climate change, addressing their design, processing and mechanical properties.

This 690-page book, which contains more than 250,000 words, 257 figures and 31 tables, delves into the fundamentals, processing, mechanical properties, applications, and key roles of these titanium alloys and lattice structures in sustainable engineering. On the one hand, this book covers the latest advances in titanium alloys (such as Ti-6Al-4V, beta-type titanium alloys, NiTi alloys, antibacterial titanium alloys, high-strength low-yield ratio titanium alloys), titanium matrix composites, their surface modifications (e.g. by friction stir processing/welding, micro-arc oxidation, electroshocking treatment, etc.), their impact in daily life, industrial sectors, and latest research trends. On the other hand, this book explores the fascinating world of additive manufacturing (or known as 3D printing) and lattice structures, covering the structure, design, 3D printing (e.g. by laser additive manufacturing, powder bed fusion, directed energy deposition), mechanical properties and their practical applications in real-world engineering. It is our aspiration that this book will not only attract readers but also inspire them to understand the current state of high-performance titanium alloys and lattice structures as well as 3D printing.

We sincerely thank the authors for their valuable contributions and the editors of the publisher for their meticulous and constructive comments. Finally, we would like to thank our families for their patience and support during the time we worked on this book.

Yuhua LI
Xi'an University of Science and Technology
Lai-Chang ZHANG
Edith Cowan University

CONTRIBUTORS

Chapter 1: Categorization and Metallurgy of Titanium Alloys
Lai-Chang ZHANG, Hongyi MA
School of Engineering, Edith Cowan University, Australia
Yuhua LI
Xi'an University of Science and Technology, China

Chapter 2: Principles of Heat Treatment in Titanium Alloys
Dingmeng XU, Peng CAO
The University of Auckland, New Zealand

Chapter 3: Beta-type Titanium Alloys
Xin WANG, Yujie YUAN, Lai-Chang ZHANG
School of Engineering, Edith Cowan University, Australia
Yuhua LI
Xi'an University of Science and Technology, China

Chapter 4: NiTi Alloys
Yuhua LI
Xi'an University of Science and Technology, China
Xin WANG, Yujie YUAN, Lai-Chang ZHANG
School of Engineering, Edith Cowan University, Australia

Chapter 5: Antibacterial Copper-Bearing Titanium Alloys
Kunmao LI
Guizhou Normal University, China
Shengfeng ZHOU
Jinan University, China
Lai-Chang ZHANG
School of Engineering, Edith Cowan University, Australia

Chapter 6: High Strength and Low Yield Ratio Titanium Alloys
Diao-Feng LI, Chun-Guang BAI, Zhi-Qiang ZHANG, Nan LI, Rui YANG
Institute of Metal Research, Chinese Academy of Sciences, China

Chapter 7: Titanium Matrix Composites
Qingsong MEI, Xinlu WANG
Wuhan University, China

Chapter 8: Laser Additive Manufacturing of Titanium Alloys
Chaolin TAN
*Singapore Institute of Manufacturing Technology (SIMTech), Agency for Science, Technology and Research (A*STAR), Singapore*
Jinlong SU
Department of Mechanical Engineering, National University of Singapore, Singapore

Chapter 9: Mechanical Performance of Beta Ti-Nb Based Alloys Produced by Laser Powder Bed Fusion
Jincheng WANG
School of Engineering, Edith Cowan University, Australia
The University of Western Australia, Australia
Yuhua LI
Xi'an University of Science and Technology, China
Yujing LIU
Yuhua Institute of Advanced Materials, China
Baoji Xigong Titanium Alloy Products Co. Ltd, China
Lai-Chang ZHANG
School of Engineering, Edith Cowan University, Australia

Chapter 10: Directed Energy Deposition of Titanium Alloys
Hua TAN, Wei FAN
Northwestern Polytechnical University, China
Fengying ZHANG
Chang'an University, China

Chapter 11: Microstructure Manipulation of Ti-6Al-4V during Additive Manufacturing
Zhonggang SUN, Guoqing DAI
Nanjing Tech University, China

Chapter 12: Titanium Lattice Structures
Xin WANG, Yujie YUAN, Lai-Chang ZHANG
School of Engineering, Edith Cowan University, Australia
Chengliang YANG
Department of Orthopedics, Affiliated Hospital of Youjiang Medical University for Nationalities, China
Guangxi Key Laboratory for Biomedical Materials Research, China
Yuhua LI
Xi'an University of Science and Technology, China

Chapter 13: Titanium Alloy Graded Lattice Structures
Lei YANG, Jiefei HUANG, Hao ZHOU
Wuhan University of Technology, China

Chapter 14: Friction Stir Processing/Welding of Titanium Alloys: Process, Microstructure and Properties
Yuting LV, Yan WANG, Yulong SHI, Wentang DENG, Wenlong XIE, Xiao KONG
Shandong University of Science and Technology, China

Chapter 15: Micro-Arc Oxidation of Titanium Alloys and Their Applications as Biomaterials
Fengcang MA, Ping LIU, Xiaohong CHEN
School of Materials and Chemistry, University of Shanghai for Science and Technology, China

Chapter 16: Electroshocking Treatment of Titanium Alloys
Jian ZHOU, Chaoyi DING, Chang LIU, Yan WEN, Lechun XIE
State Key Laboratory of Superalloy and Application Technology, Wuhan University of Technology, Wuhan 430070, China
Hubei Key Laboratory of Advanced Technology for Automotive Components, Wuhan University of Technology, Wuhan 430070, P.R. China

CHAPTER 1

CATEGORIZATION AND METALLURGY OF TITANIUM ALLOYS

LAI-CHANG ZHANG, YUHUA LI AND HONGYI MA

1.1 Crystal structure of Ti alloys

Titanium (Ti), found in subgroup IV of the periodic table, is classified as a transition metal, known for its versatility and importance in various industries. The mass number of Ti is 47.867, and it has an atomic number of 22, indicating the presence of 22 protons in its nucleus. The electronic structure of Ti is represented as $1s^2 2s^2 2p^6 3s^2 3p^6 3d^2 4s^2$, which highlights its place among the transition elements with partially filled d-orbitals, giving it unique chemical properties. With a density of approximately 4.51 g/cm^3, Ti is both lightweight and strong, making it ideal for structural applications.

Ti is relatively abundant in the Earth's crust, ranking ninth among the 112 known chemical elements, which reflects its significant presence in nature (Leyens, et al., 2006). Furthermore, it is the fourth most abundant element among structural metals, following iron, aluminum, and magnesium. This abundance is why Ti is used extensively in aerospace, medical implants, and various alloys that demand a combination of strength, corrosion resistance, and low weight.

Despite its abundance, Ti is rarely found in pure form due to its high reactivity, which makes it usually bonded with other elements, such as oxygen in minerals like rutile and ilmenite. The extraction of pure Ti metal is energy-intensive, often requiring processes such as the Kroll process, which involves the reduction of Ti tetrachloride with magnesium. This contributes to the relatively high cost of Ti compared to other metals, despite its desirable physical properties.

Ti is an allotropic element, meaning it can exhibit multiple crystal structures under different conditions (Donachie, 2000). These structures, or allotropes, exist only within specific temperature ranges, and any change in temperature can lead to a transformation between crystal forms, a process governed by what is referred to as the "transus temperature." At standard atmospheric pressure, pure Ti has two distinct isomers, with a transus temperature around 882°C.

As illustrated in Fig. 1-1(a), when below the transus temperature, pure Ti adopts a hexagonal close-packed (hcp) crystal structure, which is commonly referred to as the α phase. This phase is characterized by its excellent corrosion resistance and high strength, making it suitable for a variety of engineering applications.

In contrast, when the temperature rises above the transus temperature, the crystal structure of Ti undergoes a transformation, as shown in Fig. 1-1(b). It changes into a body-centred cubic (bcc) configuration, known as the β phase. This phase offers higher ductility compared to the α phase, which allows for improved formability and processing, especially during high-temperature manufacturing techniques. The β phase, however, is only stable at elevated temperatures and thus transitions back to the α phase upon cooling below the transus temperature.

The basic properties and characteristics of these two crystal structures are summarized in Table 1-1. The α and β phases are critical to the unique capabilities of Ti alloys, as careful control of temperature and phase composition can yield tailored properties for specialized applications, such as aerospace, biomedical devices, and high-performance structural components.

The Burgers relationship governs the crystal orientation between the α and β phases during phase transformation, expressed as $<111>_{\beta} // <1120>_{\alpha}$ and $(110)_{\beta} // (0001)_{\alpha}$ (Banerjee, et al., 2010), which can be seen in Fig. 1-1(c). Furthermore, Fig. 1-2(a) illustrates that the transformation from the bcc to hcp structure induces slight atomic distortion, resulting from differences in the distances between basal planes of the hcp and bcc crystal structures.

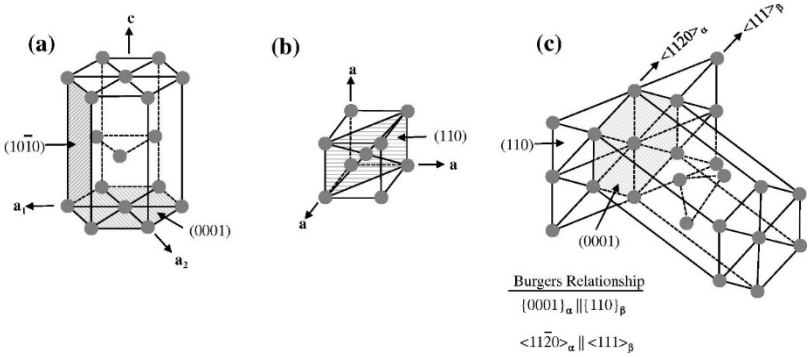

Fig. 1-1 Schematic diagram of (a) hcp and (b) bcc crystal structure; (c) Burgers relationship in the phase transformation of the α and β phases in Ti alloys (Reproduced from Beladi, et al. (2014) with permission. Copyright (2014), Elsevier).

Table 1-1 The basic crystal information of hcp and bcc structures.

Structure	*C*	*N*	*P*	*NS*	*SD*
hcp	12	6	74%	3	a
bcc	8	2	68%	12	0.87a

C - coordination number, N - number of atoms in each unit cell, P - packing density, NS – number of slip system per unit cell, SD - shortest interatomic distance, a - lattice constant.

The various crystal structures of Ti are known to exhibit unique properties. Only three slip systems are found in the hcp structure, whereas the bcc structure has twelve. Generally, having more slip systems promotes plastic deformation. Additionally, the shortest interatomic distance in the hcp structure is 1a, while it is 0.87a in the bcc structure. Consequently, more energy must be consumed to induce plastic deformation in the hcp structure. The hcp structure is typically recognized for its excellent creep resistance, while superior ductility is demonstrated by the bcc structure.

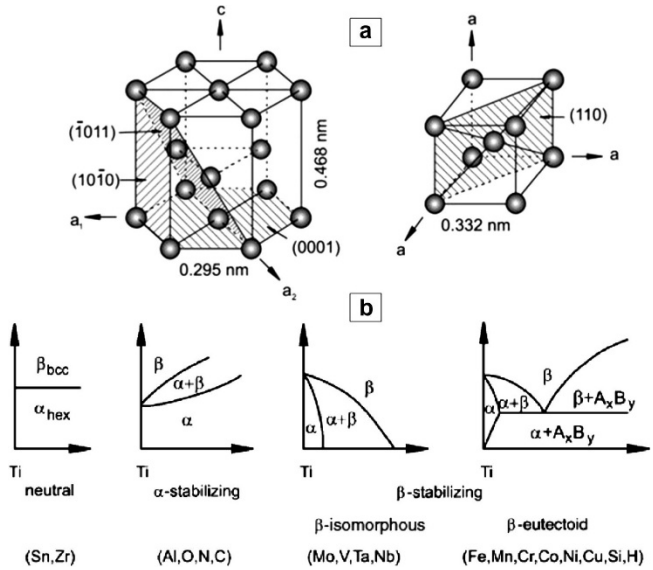

Fig. 1-2 (a) The schematic diagram shows atomic distortion during the phase transformation between the α and β phases of Ti alloys; (b) The influences of alloying elements concentrations for the phase diagrams of Ti alloy (Reproduced from Banerjee, et al. (2013) with permission. Copyright (2013), Elsevier).

For nearly all Ti alloys, alloying serves as the fundamental technical approach to enhance their overall performance. The content of alloying elements significantly influences phase transformations (Haghighi, et al., 2015). As depicted in Fig. 1-2(b), alloying elements can be classified into three categories based on their effect on the transus temperature of Ti alloys: neutral elements, β stabilizers, and α stabilizers. Typically, α stabilizers increase the allotropic transus temperature and create a two-phase region. Among the α stabilizers, aluminum (Al) plays the most crucial role, as it acts as a substitutional element with relatively high solubility, which subsequently raises the allotropic transus temperature of Ti alloys. Additionally, some interstitial elements such as carbon (C), oxygen (O), and nitrogen (N), along with rare-earth elements like boron (B), germanium (Ge), and gallium (Ga), are also frequently utilized as α stabilizers. To assess the impact of α stabilizers in multi-component Ti alloys, the Al equivalent (Al_{eq}) is often employed, which can be calculated using Equation (1):

$$[Al]wt\% = [Al] + 0.33[Sn] + 0.17[Zr] + 10[O + C + N] \qquad (1)$$

Generally, maintaining the Al equivalent (Al_{eq}) below 9 wt% in Ti alloys is necessary to prevent the formation of brittle precipitates such as Ti_3Al and $TiAl_2$.

β stabilizers have the effect of lowering the allotropic transus temperature in Ti alloys. These β stabilizers are typically divided into two categories: β-eutectic and β-isomorphous elements. Isomorphic elements, including molybdenum (Mo), vanadium (V), tantalum (Ta), and niobium (Nb), exhibit greater solubility in Ti alloys due to their ability to form solid solutions with Ti. On the other hand, eutectic elements—such as hydrogen (H), silicon (Si), copper (Cu), chromium (Cr), nickel (Ni), iron (Fe), cobalt (Co), and manganese (Mn)—can only form intermetallic compounds with Ti. As a result, isomorphic elements are generally considered more crucial for enhancing the properties of Ti alloys compared to eutectic elements. The effect of β stabilizers, comprising multiple alloying components, on Ti alloys is commonly quantified through the Mo equivalent (Mo_eq) using Equation (2):

$$[Mo]eq = [Mo] + 0.2[Ta] + 0.28[Nb] + 0.4[W] + 0.67[V] + 1.25[Cr] + 1.25[Ni] + 1.7[Mn] + 1.7[Co] + 2.5[Fe] \quad (2)$$

To effectively stabilize the β-phase, the Mo equivalent (Mo_eq) must typically exceed 10 wt%. This ensures that the β-phase remains in Ti alloys even after the quenching process.

Unlike α and β stabilizers, neutral elements generally do not impact phase transformations but play an important role in enhancing the strength of Ti alloys. Zirconium (Zr) and tin (Sn) are common neutral elements used in Ti alloys. The main contribution of neutral elements lies in refining grain size and improving the microstructure of the alloy, thereby enhancing its overall mechanical properties. Moreover, these elements have a minimal impact on the crystal structure of Ti alloys, meaning they provide strengthening effects without compromising the stability of the alloy's phase structure.

Zr is typically added to Ti alloys because it can form a complete solid solution with Ti and retain its strengthening effects even at high temperatures. This makes Zr an indispensable neutral element for high-temperature Ti alloys. Additionally, Zr also helps improve the corrosion resistance of Ti alloys, which is particularly beneficial for aerospace and marine engineering components that are exposed to corrosive environments.

Sn, another common neutral element, is also widely used in Ti alloys. It can effectively enhance the hardness and strength of Ti alloys while maintaining good ductility and toughness. The addition of tin significantly

improves the creep resistance of Ti alloys at moderate temperatures, which is important for applications requiring high endurance strength, such as aerospace engine components and industrial gas turbine blades.

Furthermore, the addition of neutral elements to Ti alloys can prevent the formation of brittle phases that might occur due to the excessive addition of α or β stabilizers. The optimal concentration of these neutral elements must be precisely controlled to ensure that the alloy maintains both excellent mechanical properties and good toughness and resistance to fracture under various harsh conditions. The unique role of neutral elements makes them crucial in the design of Ti alloy compositions, especially for alloys that need to meet the dual requirements of high strength and good processing performance.

1.2 Classification of titanium alloy

Ti alloys are commonly classified into α-type, near α-type, α+β type, metastable β-type, and stable β-type, based on the type and concentration of alloying elements. These different types of Ti alloys are illustrated schematically through a three-dimensional phase diagram (Fig. 1-3). The performance characteristics of Ti alloys vary across the different types, meaning that the choice of a specific alloy type generally depends on factors like operational conditions, cost, required functionality, and other considerations.

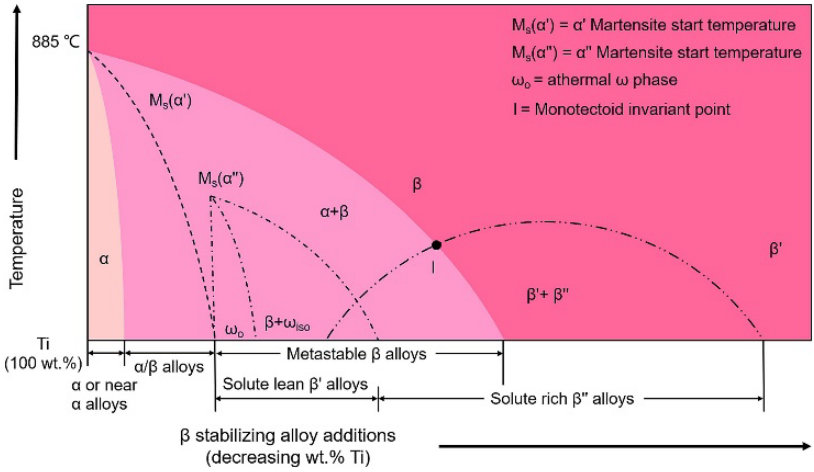

Fig. 1-3 The phase diagram of different types of Ti alloys (Reproduced from Cui, et al. (2024) with permission. Copyright (2024), Elsevier).

α-type Ti alloys primarily consist of different grades of commercially pure Ti (CP-Ti), unlike other Ti alloys that only incorporate α-stabilizing elements (Geetha, et al., 2009). Due to their hexagonal close-packed (hcp) crystal structure, α-type Ti alloys generally do not exhibit a ductile-to-brittle transition temperature, which makes them suitable for applications across a wide range of temperatures—from high temperatures to cryogenic conditions. Additionally, with fewer available slip systems inherent to the hcp structure, these alloys demonstrate excellent creep resistance and favorable fatigue characteristics (Geetha, et al., 2009). The weldability of α-type Ti alloys is another significant advantage, as their properties are minimally affected by heat treatment, resulting in reliable weld integrity (Donachie, 2000). They also offer remarkable corrosion resistance, making them an excellent choice for applications in harsh environments (Lütjering, et al., 2007). Despite these advantages, α-type Ti alloys have limitations. Their hcp crystal structure makes them difficult to strengthen via heat treatment, which results in relatively low inherent strength. Moreover, compared to (α+β)-type and β-type Ti alloys, α-type Ti alloys have a narrower temperature range for forging and are characterized by lower forgeability. As a result, during forging, more frequent reheating and smaller incremental deformation steps are necessary to shape these alloys effectively. Due to these properties, α-type Ti alloys are typically utilized in specialized applications where their superior resistance to high temperatures and corrosion is required. Examples include heat exchangers and pressure pipes in the chemical industry, where the combination of corrosion resistance, weldability, and adequate strength is highly valued.

Near α-type Ti alloys typically contain a small proportion (1-2%) of β-stabilizing elements in addition to α-stabilizers (Geetha, et al., 2009). As a result, the microstructure of near α-type Ti alloys primarily consists of the α phase with a minor presence of the β phase, typically in the range of 5-10%. While both near α-type and α-type Ti alloys share similar mechanical properties, near α-type alloys offer enhanced creep resistance and excellent corrosion resistance, albeit at the cost of reduced forgeability. One key difference between these two types lies in the influence of the β phase present in near α-type alloys. The small amount of β phase allows near α-type alloys to be strengthened through heat treatment, which is not possible for fully α-type alloys (Donachie, 2000). This additional strengthening capability makes near α-type Ti alloys more versatile for applications demanding higher mechanical performance. Due to these properties, near α-type Ti alloys are frequently employed in high-temperature structural applications within the aviation industry. They are particularly useful for components such as compressor discs and turbine engine parts, where a

combination of high-temperature strength, resistance to creep, and corrosion resistance is critical to ensure the reliability and durability of aerospace engines.

(α+β) Ti alloys typically contain between 4-6 weight percent (wt.%) of β-stabilizers and exhibit a β-phase volume fraction ranging from 5% to 40% (Leyens, et al., 2006). The presence of a significant β-phase provides these alloys with moderate strength at elevated temperatures and exceptional strength at ambient conditions [10]. Furthermore, (α+β) Ti alloys can undergo heat treatment to further improve their mechanical properties, as such treatment modifies the proportion of α and β phases within the alloy (Bai, et al., 2017, Cohen, 1967, Dai, et al., 2016). Suitable solution treatment and aging processes can enhance the strength of (α+β) Ti alloys by as much as 30% to 50% (Chen, et al., 2015). In addition to their excellent mechanical properties, (α+β) Ti alloys also demonstrate remarkable corrosion resistance. This resistance is primarily due to the formation of a stable Ti dioxide (TiO_2) or hydroxide (TiO_2/OH) layer on the surface, which protects the underlying material from corrosion (Narayan, 2009). These characteristics make (α+β) Ti alloys highly versatile and contribute to their widespread use across industries. The importance of (α+β) Ti alloys is evident in their extensive commercial use; more than half of the Ti alloys utilized in various sectors are of the (α+β) type. One of the most well-known (α+β) Ti alloys is Ti-6Al-4V, which has found widespread application in both the biomedical field and aerospace industry due to its excellent balance of strength, corrosion resistance, and biocompatibility (McAndrew, et al., 2018).

Metastable β-type Ti alloys typically contain between 10-15 weight percent (wt.%) of β-stabilizing elements, which allow them to remain entirely in the β-phase at room temperature after rapid quenching. During this quenching process, no martensitic transformation occurs, which contributes to their stability in the metastable state. The presence of twelve slip systems gives metastable β-type Ti alloys excellent formability, making them suitable for applications where complex shapes are required. Heat treatment of metastable β-type Ti alloys can result in the precipitation of more than 50% of the α-phase in the microstructure, which significantly enhances the material's properties. These alloys can achieve high tensile strength exceeding 1400 MPa, while also providing high toughness and excellent resistance to fatigue. Furthermore, they offer outstanding corrosion resistance, a relatively low Young’s modulus, and exceptional biocompatibility, making them ideal for biomedical applications. Despite these advantages, the production of metastable β-type Ti alloys can be challenging due to their sensitivity to impurities, particularly oxygen, which can compromise their mechanical properties. Additionally, the unstable

nature of the β phase limits the use of these alloys to temperatures below 300°C. Given these characteristics, metastable β-type Ti alloys are predominantly employed in the biomedical field, where their favorable combination of mechanical properties, biocompatibility, and corrosion resistance is highly valued.

Stable β-type Ti alloys generally contain over 30 wt.% β-stabilizing elements, allowing them to maintain stability in the β-phase at room temperature. These stable β-type alloys exhibit remarkable ductility, attributed to the stability of their single-phase microstructure. Additionally, due to the absence of a micro-galvanic effect between different phases, they offer excellent resistance to corrosion. Currently, only a limited number of stable β-type Ti alloys have been developed. Typical examples include Ti-32Mo, Ti-35V-15Cr, and Ti-25V-15Cr-0.2Si, among others. Ti-32Mo is often utilized in the chemical industry because of its outstanding corrosion resistance. On the other hand, Ti-35V-15Cr and Ti-25V-15Cr-0.2Si alloys are well-suited for high-temperature applications, as they retain stability and possess excellent flame resistance, allowing their use at temperatures up to around 500°C for prolonged durations. Despite these advantages, stable β-type Ti alloys also come with certain drawbacks, including high specific gravity and challenges in the melting process, which can complicate their production and limit their broader application.

1.3 Various phases of Ti alloys.

Different production conditions can lead to the formation of various equilibrium or non-equilibrium phases in Ti alloys. Typically, the equilibrium phases in Ti alloys consist of the α and β phases, which primarily transform via diffusion-controlled pathways. Conversely, when diffusion is restricted, non-equilibrium phases can form, such as hexagonal martensite (α'), orthorhombic martensite (α"), and the ω phase, among others. These non-equilibrium phases arise under rapid cooling conditions where diffusion is limited, altering the microstructure of the alloy.

1.3.1 Equilibrium phase - α phase

One of equilibrium phases in Ti alloys is the α phase, whose crystal structure aligns with that found in pure Ti. This α phase exists as a disordered solid solution composed of Ti atoms and solute elements. The atomic positions of the α phase are located at (0,0,0), (1/3,1/3,1/2), with the corresponding space group being (P63/mmc). However, the introduction of alloying elements leads to a modification of the lattice constant of the α phase. Upon

slow cooling of Ti alloys from the β phase region, solute atoms are able to diffuse, resulting in the gradual formation of regions with reduced concentrations of β stabilizers. This phenomenon favors the nucleation of the α phase. The α phase initiates at the grain boundaries of the β phase and continues growing until colonies of α plates are established along these boundaries, forming what is known as αGB, as illustrated in Fig. 1-4. Following this, α-phase plates begin to nucleate at the interface between α_{GB} and the β phase, extending further into the β phase. These adjacent α plates, separated by the β phases, exhibit identical crystal orientations. Ultimately, the growth of different colonies of α plates is mutually constrained, giving rise to basket weave microstructure. The α phase present in this basket weave microstructure is commonly referred to as α_{WGB}. The primary strengthening mechanism of Ti alloys is attributed to the restriction of dislocation movement caused by the interfaces between the α plates and β phases. Consequently, controlling and predicting the size, morphology, and spatial distribution of the α phase are of paramount importance in determining the final properties of Ti alloys.

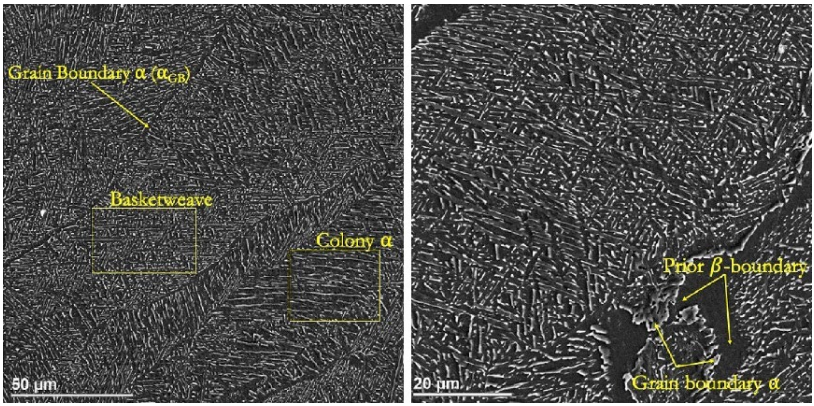

Fig. 1-4 Typical structures of α_{GB} (Reproduced from Dharmendra, et al. (2020) with permission. Copyright (2020), Elsevier).

1.3.2 Non-equilibrium phases β', α', α'' and ω phases

When the cooling rate is low, the transformation of the β phase into the α phase occurs through diffusion. Conversely, as the cooling rate increases, the diffusion-driven transformation from β to α phases is delayed, potentially resulting in the formation of non-equilibrium phases from the β phase. This process, illustrated in Fig. 1-3, is influenced by the

concentration of β stabilizers in Ti alloys, which determines the specific types of non-equilibrium phases that can emerge. As the β stabilizer content rises, martensitic transformations may induce the formation of α' or α" phases from the β phase when Ti alloys are rapidly quenched, crossing the martensite start temperature. If the concentration of β stabilizers approaches or slightly surpasses the upper limit for α" phase formation, the ω phase is likely to develop in Ti alloys. With further increases in β stabilizer content, the β phase may subsequently transform into a combination of β and β' phases.

1.3.3 Phase transformation of β→α', α''

When Ti alloys undergo rapid cooling, non-diffusion martensitic transformations lead to the formation of α' and α" phases. The α' phase adopts a hexagonal crystal structure (hex) and maintains the Burgers relationship with the β phase, following the orientations $<111>_{\beta}$ // $<1120>_{\alpha'}$ and $(110)_{\beta}$ // $(0001)_{\alpha'}$. The α" phase, on the other hand, exhibits an orthorhombic crystal structure is defined by specific atomic positions: (0,0,0), (1/2, 1/2, 0), (0, 1-2y, 1/2), and (1/2, 1/2-2y, 1/2). Although the lattice constants of the α' and α phases are nearly identical, the α' phase is characterized by being a supersaturated solid solution, rich in solute elements. The transformation mechanisms of β→α and β→α' differ due to variations in cooling rates. Under slow cooling, the β phase can gradually transition to the α phase through diffusion. Conversely, if the cooling rate is extremely high, solute elements do not have adequate time to diffuse, resulting instead in the formation of the α' phase. This difference in phase formation underlines the critical role of cooling speed in determining the microstructure of Ti alloys.

With the increasing concentration of an alloying element in Ti alloys, the transformation from the body-centered cubic (bcc) to the hexagonal structure ("bcc → hex") becomes increasingly impeded, which results in the formation of martensitic α" phases. Compared to the α' martensite phase, the deformation associated with the α" phase is notably smaller. This reduced deformation is attributed to the nature of the structural changes involved in forming α", which leads to less lattice distortion and a more stable configuration under certain conditions.

Furthermore, it is noteworthy that the transformation to the α" martensitic phase can also be stress-induced in some Ti alloys. This means that under applied mechanical stress, the β phase can transform into the α" phase, providing the material with unique deformation capabilities that may be advantageous in certain engineering applications. The ability to induce

martensitic transformation through stress is particularly significant in alloys used for shape memory or superelastic properties, where stress-induced phase transformations enable materials to recover their original shape after deformation.

According to the phenomenological theory of martensite, the phase transformation pathways for both α' and α" martensitic phases follow a similar sequence involving three primary steps. The first step involves Bain distortion, during which the cubic crystal structure transforms into orthorhombic and hexagonal crystal structures. Bain distortion is essentially a homogeneous deformation that alters the original cubic unit cell into different crystallographic forms, leading to the formation of martensitic structures. This initial transformation provides the fundamental framework for the development of the martensitic phases.

The second step involves lattice-invariant deformation, which occurs either by twinning or slipping within the crystal structure. Lattice-invariant deformation is a critical process that allows the material to accommodate the overall shape change associated with the phase transformation without causing excessive stress within the crystal. Twinning and slip are mechanisms that help maintain coherency between transforming regions, ensuring that the crystal structure remains intact and reducing the likelihood of defect formation.

The final step in the transformation pathway involves a shift in the spaced (110) crystal planes along the $[1\bar{1}0]$ direction. As illustrated in Fig. 1-5, this displacement plays a crucial role in determining whether the α' or α" martensitic phase is formed. Specifically, when the displacement along the $[1\bar{1}0]$ direction reaches $1/6\sqrt{2}a_{\beta}$, the α’ phase is formed, whereas when the displacement remains less than $1/6\sqrt{2}a_{\beta}$, the resulting phase is α’’. This distinction highlights the importance of the magnitude of displacement in dictating the resulting crystal structure, with subtle differences leading to markedly different phases and, consequently, different material properties.

The movement of the (110) crystal plane in the α” phase is further characterized by its 4c Wyckoff position, denoted by the value "y," which determines the extent of the displacement. The amount of movement can be quantified by the expression $(1/2\text{-}2y)\ \sqrt{2}a_{\beta}$, and the range of the y value lies between 1/4 and 1/6. This range of values represents the extent of possible shifts within the orthorhombic lattice, with significant implications for the stability and characteristics of the resulting martensitic phase. Notably, when the y value is equal to 1/4 or 1/6, the orthorhombic lattice becomes equivalent to the bcc and hexagonal close-packed (hcp) structures, respectively. This equivalence indicates that under specific conditions, the

orthorhombic phase can effectively revert to either of these more stable structures, depending on the exact value of the Wyckoff parameter.

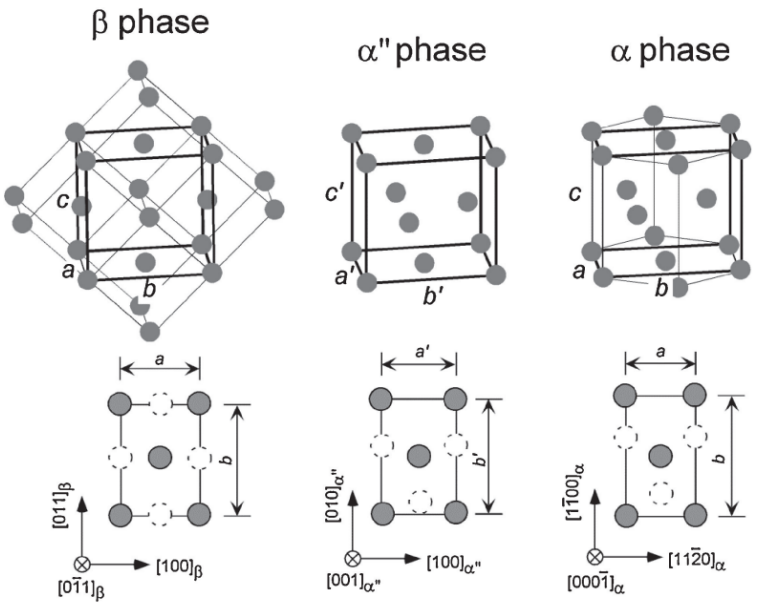

Fig. 1-5 The lattice correspondence of the transformation of "β → α',α" phases (Reproduced from Kim, et al. (2015) with permission. Copyright (2015), J-STAGE).

The lattice distortion that occurs during the β→α' phase transition can be characterized by specific directional changes: a compression of approximately 10% along $[100]_\beta$ or $[2\bar{1}\bar{1}0]_{\alpha'}$, an expansion of about 10% along $[01\bar{1}]_\beta$ or $[01\bar{1}0]_{\alpha'}$, and a smaller expansion of roughly 1% along $[011]_\beta$ or $[0001]_{\alpha'}$. In Fig. 1-6, the lattice correspondence between β and α" phases is illustrated, revealing that the α" phase experiences less lattice distortion compared to the α' phase. The degree of this lattice distortion is influenced by the lattice constant of the α" phase, which is, in turn, affected by the concentration of β-stabilizing elements.

As shown in Fig. 1-6, the lattice constants of both β and α" phases vary with the concentration of Nb in the alloy. When the Nb concentration is within the range of 22-35 atomic percent (at.%), each 1 at.% increase in Nb leads to a rise in a_β by 0.013×10^{-3} nm. Additionally, Fig. 1-7 illustrates how the lattice distortion alters in three specific directions: $[100]_\beta$, $[011]_\beta$, and $[0\bar{1}\bar{1}]_\beta$.

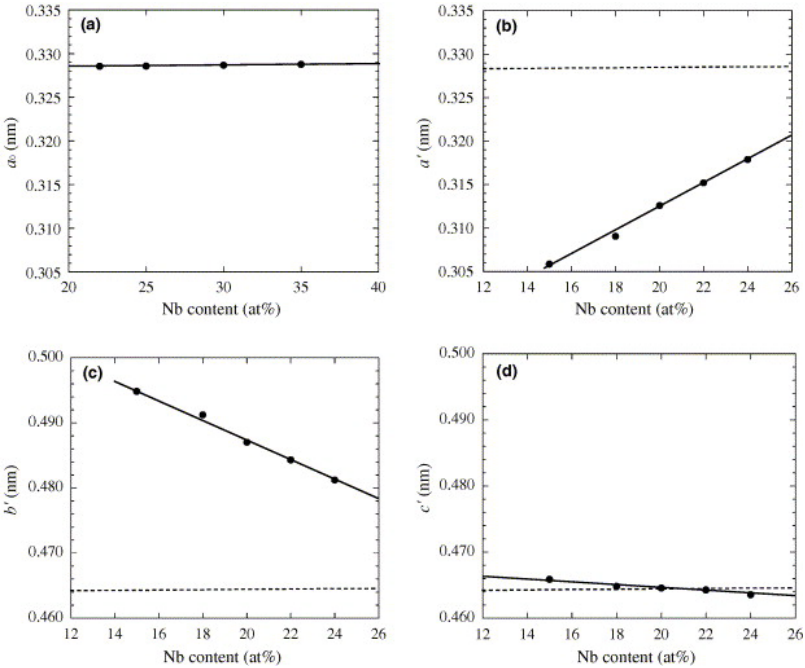

Fig. 1-6 Influence of Nb concentration on lattice constants of α" and β phases Kim, et al. (2006) with permission. Copyright (2006), Elsevier).

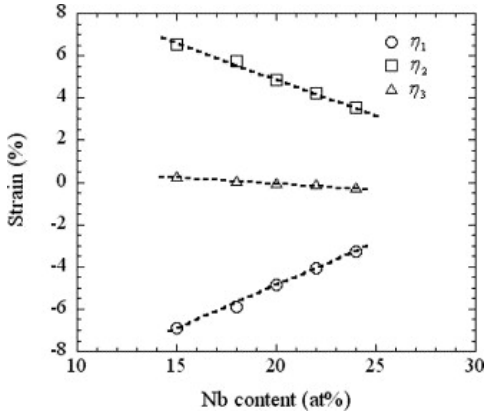

Fig. 1-7 Influence of Nb concentration on lattice strain required for the transformation of β → α" along three major axes of α" phase (Reproduced from Kim, et al. (2006) with permission. Copyright (2006), Elsevier).

Fig. 1-8 illustrates two common structural forms of the martensitic α' phase. Depending on the concentration of alloying elements, martensitic phases in Ti alloys tend to form either a block structure, typically observed in alloys with low concentrations of alloying elements, or an acicular (needle-like) structure, found in alloys with higher solid solubility. The block structure is made up of closely packed martensitic laths, with no β phase present between these laths. Conversely, the needle-like structure consists of a β-phase matrix interspersed with martensitic sheets. Notably, there is no precise alloying concentration threshold separating these two martensitic morphologies; in some Ti alloys, both structures can coexist. Since martensitic phases form through non-diffusive transformations, they generally contain solute elements in supersaturated amounts. During aging within the α+β two-phase field, excess solute elements are expelled according to the solubility limit of the alloying elements at the given temperature. For the α' block structure, this process leads to the precipitation of the β phase along dislocations, as well as at lath and twin boundaries (α'→α+β). In the case of the α'' needle-like structure, the α'' phase undergoes a continuous decomposition into regions with low and high solute concentrations, which subsequently transform into α and β phases, respectively (α''→α''lean+α''rich→α+β).

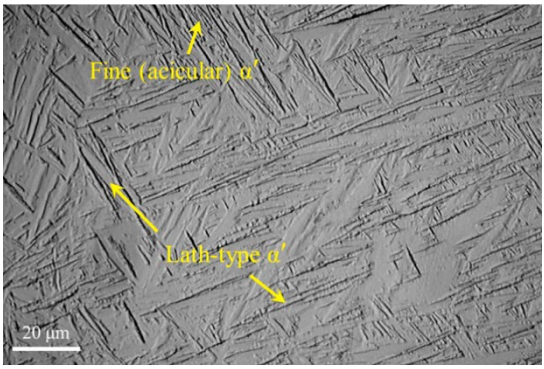

Fig. 1-8 Two typical structure types of the martensite α' phase (Reproduced from Attar, et al. (2017) with permission. Copyright (2017), Elsevier).

1.3.4 Phase transformation of β→ω

The ω phase is stable in pure Ti under high pressure but exists as a metastable phase in Ti alloys at normal pressure. Structurally, the ω phase has both a hexagonal (P6/mmm) and triangular ($P\bar{3}m1$) configuration, with

atomic positions at (0,0,0), (2/3,1/3,1/2), and (1/3,2/3,1/2) in the hexagonal structure, and (0,0,0), (2/3,1/3,1/2+z_ω), (1/3,2/3,1/2-z_ω) in the triangular configuration. The ω phase generally forms through two distinct mechanisms: the athermal ω phase appears when Ti alloys are water-cooled from the β-phase field, while the isothermal ω phase develops during aging at low temperatures (below 500°C). Additionally, transformations from β to ω phases can also be induced by applied stress or strain. The formation of the ω phase involves the collapse and merging of two out of three adjacent $(111)_\beta$ planes in the {111} plane family of the β phase into a single plane, while the remaining plane remains unchanged [9]. During this transformation, the lattice constant (z_ω) of the ω phase varies from 0 to 1/6. When z_ω equals 0, the ω phase structurally aligns with the β phase. Conversely, when z_ω reaches 1/6, the ω phase adopts a hexagonal configuration, and when z_ω is between 0 and 1/6, the structure is triangular. The orientation relationship between the ω and β phases is as follows: $(0001)_\omega // (111)_\beta$ and $<11\bar{2}0>_\omega // <110>_\beta$.

The ω_{iso} phase, which is generated through prolonged isothermal aging, typically grows to approximately 10-100 nm and assumes either an elliptical or cubic structure. This particular phase's shape is significantly influenced by the misfit strain resulting from various alloying elements. For instance, in alloys containing Ti and elements like V, Cr, Mn, or Fe—those with a low misfit volume—the ω_{iso} phase exhibits an elliptical morphology. Conversely, for alloys such as Ti-Mo or Ti-Nb, where the misfit volume is considerably higher, the ω_{iso} phase tends to adopt a cubic structure. On the other hand, the ω_{ath} phase is markedly smaller, measuring only 2-10 nm, and is uniformly dispersed throughout the β-phase matrix. Unlike the ω_{iso} phase, the ω_{ath} phase does not display a regular shape; rather, it exhibits an irregular morphology, which is typically identified through selected area electron diffraction (SAED), dark-field imaging, or high-resolution transmission electron microscopy (TEM) images. When Ti-Nb alloys are air-cooled from a high temperature of around 1000°C down to room temperature, as illustrated in Fig. 1-9, distinct diffraction spots representing the ω phase can be observed at $1/3<112>_\beta$ and $2/3<112>_\beta$ positions. With an increased Nb content, these diffraction spots gradually weaken and evolve into diffuse streaks, making it increasingly challenging to discern the precise shape of the ω phase. This particular variant is commonly referred to as the diffuse ω phase (ω_{diff}) (Hanada, et al., 1987). Research into certain Ti-TM-based metastable β-phase alloys has demonstrated that, within specific compositional ranges, these Ti alloys exhibit a negative resistance-temperature coefficient at room temperature. This effect is primarily

attributed to the lattice distortions introduced by the ω_{diff} phase, which plays a central role in generating this unique property.

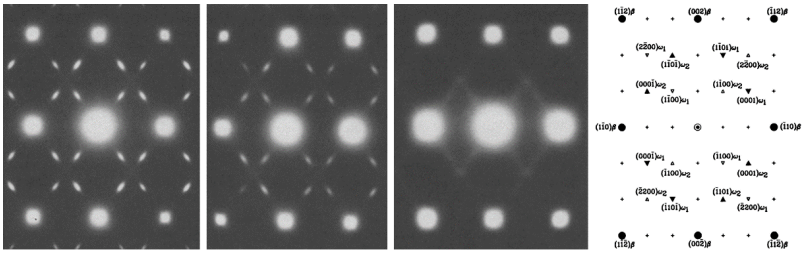

Fig. 1-9 SAED patterns of Ti-Nb alloys with various content of Nb elements air cooled from 1000℃ to room temperature (Reproduced from Moffat, et al. (1988) with permission. Copyright (1988), Spring Nature).

The ω phase, therefore, plays a crucial role in determining the ultimate properties of Ti alloys, leading to extensive research on this phase over the past five decades. The formation mechanisms of the ω phases differ notably: the ω_{ath} phase arises from the collapse of the {111} crystal planes in the β phase. In contrast, the ω_{iso} phase is produced through a two-step process. Initially, the solute elements within the β phase are redistributed via thermally activated diffusion; subsequently, the {111} planes of the β phase collapse within the solute-depleted regions (Nag, et al., 2011). Advancements in three-dimensional atom probe (3DAP) technology and high-resolution scanning transmission electron microscopy (HRSTEM) have provided deeper insights into the transformation processes between the β and ω phases. These studies have revealed phase transition mechanisms in which displacements of crystal planes are influenced by compositional variations within the β and ω phases. For example, as illustrated in Fig. 1-10, the degree of crystal plane displacement in Ti-Mo alloys shifts in alignment with the compositional gradient across the phases, emphasizing the role of composition in phase stability and transformation behavior.

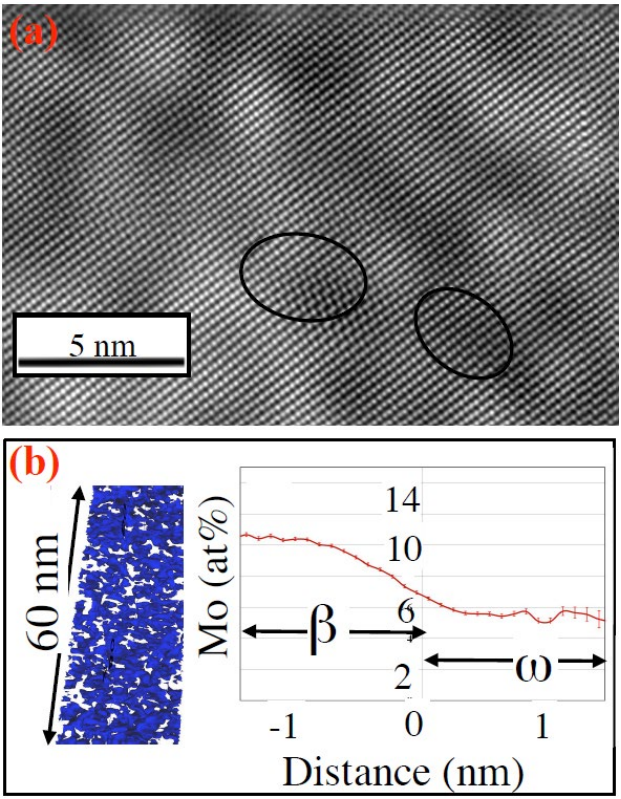

Fig. 1-10 The different degrees of crystal plane displacement in microscale solute-rich and solute-lean regions (Reproduced from Nag, et al. (2011) with permission. Copyright (2011), American Physical Society).

1.3.5 Phase transformation of β→β+β'

The transformation from β to β+β' in Ti alloys, especially those with high concentrations of β stabilizers, typically occurs under heat treatment conditions. This transformation is driven by the redistribution of solute atoms within the alloy. In this context, β represents regions rich in solute elements, while β' corresponds to areas where solute elements are sparse. The β→β+β' transformation can proceed either through a nucleation and growth process or via spinodal decomposition. When nucleation occurs, it leads to substantial variations in phase composition, which can contribute

to increased phase stability. Conversely, spinodal decomposition involves smaller compositional fluctuations within the resulting phases.

Early studies identified both β and β' phases as having a body-centered cubic (bcc) structure ($Im\bar{3}m$), with atomic sites located at (0,0,0) and (1/2,1/2,1/2). With advancements in research technology, the structural characterization of the β' phase has become more precise. It has also been observed that the β→β+β' phase transformation is not limited to Ti alloys with high β-stabilizer concentrations; other Ti alloy systems can also undergo this transformation. The β' phase in Ti alloys can be further divided into two distinct morphological types. As shown in Fig. 1-11(a), one type of β' phase appears elliptical and retains the bcc structure, consistent with earlier findings. Due to compositional differences, the lattice constant of this β' phase type varies slightly from that of the β phase. The other type of β' phase, depicted in Fig. 1-11(b), is plate-like and possesses a body-centered tetragonal (bct) structure, which has a lower symmetry compared to the bcc structure. For this bct β' phase, the lattice constants are a_β'=b_β'=3.35Å and c_β'=3.80Å, which differ from the lattice constant of the β phase, a_β=3.45Å. Although the metastable β phase structure is highly sensitive to compositional fluctuations in the alloy, there remains considerable uncertainty regarding its precise structure. High-resolution analysis methods are required to determine whether coordinated displacements of crystal planes occur during the diffusion of solute elements. Thus, the characteristics of the β' phase in Ti alloys cannot be universally defined across all systems, underscoring the need for focused research on each specific alloy composition.

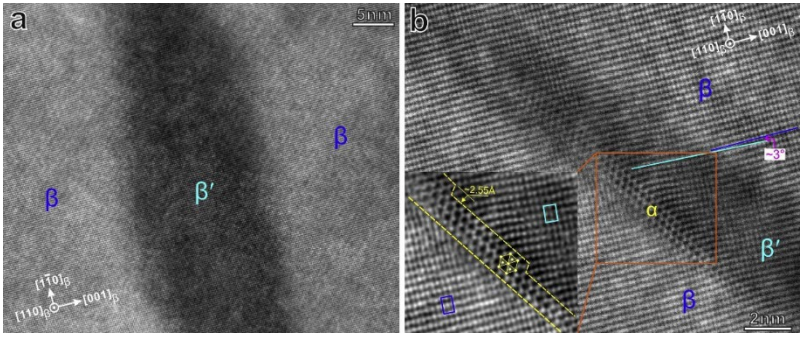

Fig. 1-11 The different shapes of β' phase in the Ti-25Nb-3Mo-3Zr-2Sn alloy; (a)elliptical (b)plate-shape (Reproduced from Zhu, et al. (2016) with permission. Copyright (2016), Elsevier).

1.3.6 Other non-equilibrium phases

In addition to phases that are in equilibrium or non-equilibrium, which may induce substantial alterations in crystal structures, attention has also been drawn to localized structural changes that occur with temperature in certain Ti alloys. This type of transformation exhibits several distinctive characteristics. Firstly, as illustrated in Fig. 1-12(a), the macroscopic crystal structure of Ti alloys retains the body-centered cubic (bcc) form, meaning that conventional X-ray diffraction (XRD) methods are unable to detect any shift in diffraction peaks before and after the transformation takes place. Secondly, as indicated in Fig. 1-12(b), throughout the transformation process, the elastic modulus of Ti alloys initially decreases and subsequently increases with a rise in temperature, with the specific temperature at which the elastic modulus reaches its lowest value shifting depending on frequency variations. Thirdly, as depicted in Fig. 1-12(c), no prominent local structural modifications are visible in the Transmission Electron Microscopy (TEM) bright field; however, weaker diffraction patterns can be discerned in Selected Area Diffraction (SAD). Lastly, as presented in Fig. 1-12(d), the presence of localized lattice distortions becomes evident in high-resolution TEM (HRTEM) images.

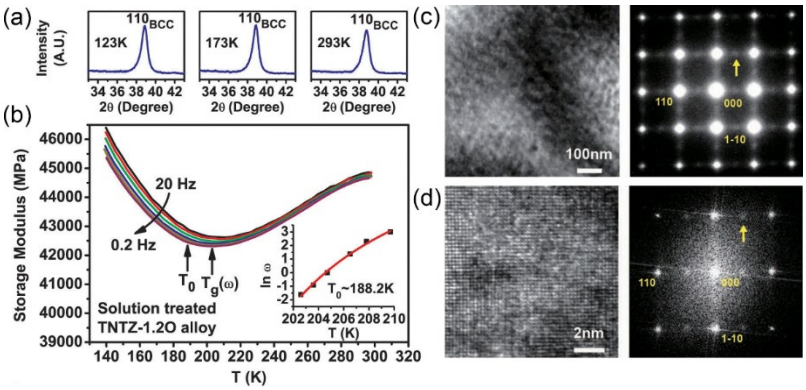

Fig. 1-12. (a) in-situ cooling XRD, (b) dynamically mechanical analysis (DMA), (c) TEM and (d) HRTEM observation of the Ti-23Nb-0.7Ta-2Zr-1.2O alloy (Reproduced from Wang, et al. (2014) with permission. Copyright (2014), Springer Nature).

As research continues to advance, a more profound understanding of localized structural transformations can be achieved. In Ti-Nb-based alloys that are enriched with oxygen elements, this type of structure is referred to